Nuclear Mathematical and Computational Sciences: A Century in Review, A Century Anew
Gatlinburg, Tennessee, April 6-11, 2003, on CD-ROM, American Nuclear Society, LaGrange Park, IL (2003)

A PIECEWISE LINEAR FINITE ELEMENT BASIS WITH APPLICATION TO PARTICLE TRANSPORT

Hiromi G. Stone and Marvin L. Adams
Department of Nuclear Engineering, Texas A&M University
3133 TAMU
College Station, TX 77843-3133
hiromi@tamu.edu; mladams@tamu.edu

ABSTRACT

We introduce piecewise linear basis functions that have very attractive properties for finite element approximations of partial differential equations on unstructured grids, including grids of arbitrary polygons (2D) or polyhedrons (3D). We apply discontinuous versions of these basis functions to the particle transport equation on arbitrary grids. We analyze the behavior of the resulting solution in various limits of interest. We provide numerical results from test problems in 2D problems with arbitrary quadrilateral cells and compare against results from established methods on arbitrary and rectangular grids. We conclude that the piecewise linear basis functions are very promising and could lead to an improvement in the state of the art of particle transport on unstructured grids.

Key Words: finite element, discontinuous, unstructured grid, polygons, discrete ordinates

1. INTRODUCTION

The motivation for this work is the need to solve differential equations on non-orthogonal grids. Some common grid choices for two-dimensional/three-dimensional problems, along with some available options for simple finite element method (FEM) basis functions, are:

- Triangles/tetrahedra: Many options, including linear
- Quadrilaterals/hexahedra:
  (1) Bilinear/Trilinear on mapped square/cube, or
  (2) Wachspress's rational functions [1]
- General polygons/polyhedrons: only Wachspress's rational functions

Here we present new FEM basis functions that are alternatives to Wachspress's rational (WR) functions and that can be applied to polygons and polyhedrons. Each basis function is piece-wise linear (PWL). Some characteristics of PWL functions and WR functions are:

- Both can be applied to essentially arbitrary polygons/polyhedrons.
- WR functions can be applied to cells with simple curved surfaces ("polycons"); PWL cannot.
- PWL integrals are simple to compute analytically; WR must be done numerically.
- WR functions have continuous derivatives inside cells; PWL functions do not.
- Both have unknowns only at vertices (same unknown count).

The PWL FEM can be applied to a wide variety of differential equations. For example, continuous PWL functions are well suited for solving diffusion problems. Here we study a PWL discontinuous (PWLD) method for particle transport.

Our previous study of a PWLD method has shown that on problems with rectangular grids, PWLD performs as well as well as the well-established bilinear discontinuous (BLD) method [2]. In this work we study PWLD applied to non-rectangular grids. We analyze the method for general polygonal grids in 2D, and numerically test it on grids with quadrilateral cells.

2. PWL BASIS FUNCTIONS

To define PWL basis functions for two-dimensional polygons, we first divide each polygonal cell into triangular "side" sub-cells. Each triangular side is defined by two adjacent vertices and the within-cell point "*c*." The coordinates of *c* are weighted averages of the vertex coordinates:

$$x_c = \sum_{j=1}^{J_c} \alpha_{c,j} x_j,\ y_c = \sum_{j=1}^{J_c} \alpha_{c,j} y_j, \quad \text{where} \sum_{j=1}^{J_c} \alpha_{c,j} = 1 \quad \text{and} \quad J_c = \text{number of vertices in cell } c. \quad (1)$$

Then the basis function at vertex *j* of cell *c* is defined as

$$b_{c,j}(x,y) = t_{c,j}(x,y) + \alpha_{c,j} t_c(x,y) \quad (2)$$

where the "*t*" functions are standard linear functions on triangles: $t_{cj}(x,y)$ is unity at vertex *j*; zero at *j*-1, *j*+1, and *c*; and zero in all triangular sides that do not touch vertex *j*. The function $t_c(x,y)$ is unity at *c* and zero at each vertex. The parameters $\{\alpha_{c,j}\}$ are arbitrary positive weights as far as the PWL formalism is concerned.

We will describe the construction of PWL basis functions for specific geometries in more detail in latter subsections

2.1. PWL Discontinuous (PWLD) FEM for Transport with Rectangular Grids

Here we present PWL basis functions on a rectangular grid and their application to particle transport problems. We refer to Figure 1 for the notation and location of points in a rectangular cell [3]. Here the coordinates of the within-cell point "*c*" is taken to be the average of four vertices, i.e. $\alpha_{c,j} = 1/4$ for all *j* in equation (1). Figure 1 also shows triangular side sub-cells.

We use Galerkin weighting for PWLD FEM. Then PWLD basis and weight functions can be written as the following:

$$w_{c,j} = b_{c,j}(x,y) = t_{c,j}(x,y) + \frac{1}{4} t_c(x,y), \quad j = 1,\ldots,4. \quad (3)$$

Figure 2 illustrates a PWLD basis function on a one-cm by one-cm rectangular cell, showing the basis function with support point at (0,0).

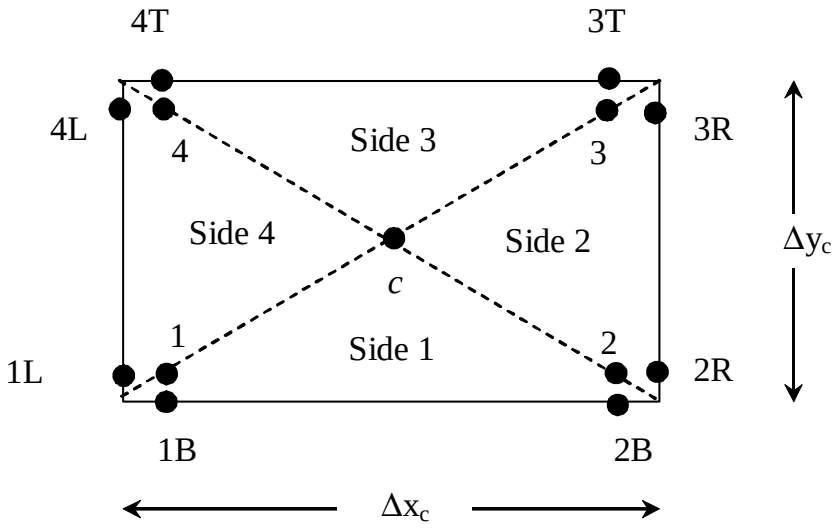

Figure 1. Location of points in rectangular cell *c*.

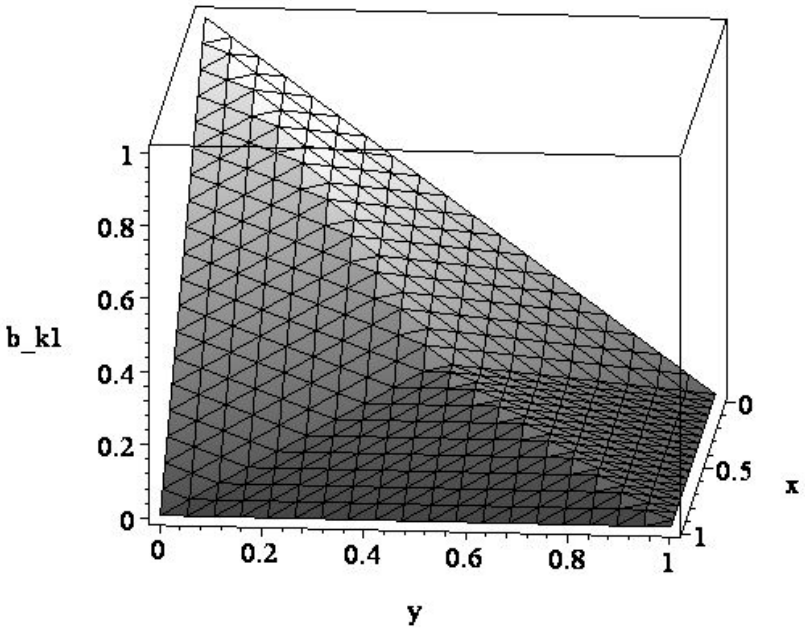

Figure 2. Illustration of a PWL basis function on a rectangular grid.

The general discontinuous finite element (DFEM) transport equation is [2]:

$$\int_{\partial V_c} d^2 r w_{ci}(\mathbf{r})\mathbf{n}\bullet\boldsymbol{\Omega}\Psi(\mathbf{r},\boldsymbol{\Omega}) + \sum_{j=1}^{J_c}\psi_{cj}\int_{V_c} d^3 r\left[-b_{cj}(\mathbf{r})\boldsymbol{\Omega}\bullet\nabla w_{ci}(\mathbf{r}) + w_{ci}(\mathbf{r})\sigma_t b_{cj}(\mathbf{r})\right] = \int_{V_c} d^3 r\, w_{ci}(\mathbf{r})q(\mathbf{r}). \tag{4}$$

Then PWLD FEM equation on a rectangular cell can be written:

$$\frac{\mu\Delta y}{6}\begin{bmatrix}-2\psi_{1L}-\psi_{4L}\\ 2\psi_{2R}+\psi_{3R}\\ \psi_{2R}+\psi_{3R}\\ -\psi_{1L}-2\psi_{4L}\end{bmatrix}+\frac{\mu\Delta y}{12}\begin{bmatrix}2&2&1&1\\-2&-2&-1&-1\\-1&-1&-2&-2\\1&1&2&2\end{bmatrix}\begin{bmatrix}\psi_1\\\psi_2\\\psi_3\\\psi_4\end{bmatrix}+\frac{\eta\Delta x}{12}\begin{bmatrix}2&1&1&2\\1&2&2&1\\-1&-2&-2&-1\\-2&-1&-1&-2\end{bmatrix}\begin{bmatrix}\psi_1\\\psi_2\\\psi_3\\\psi_4\end{bmatrix}$$
$$+\frac{\eta\Delta x}{6}\begin{bmatrix}-2\psi_{1B}-\psi_{2B}\\ -\psi_{1B}-2\psi_{2B}\\ 2\psi_{3T}+\psi_{4T}\\ \psi_{3T}+2\psi_{4T}\end{bmatrix}+\frac{\sigma\Delta x\Delta y}{96}\begin{bmatrix}11&5&3&5\\5&11&5&3\\3&5&11&5\\5&3&5&11\end{bmatrix}\begin{bmatrix}\psi_1\\\psi_2\\\psi_3\\\psi_4\end{bmatrix}=\frac{\Delta x\Delta y}{96}\begin{bmatrix}11&5&3&5\\5&11&5&3\\3&5&11&5\\5&3&5&11\end{bmatrix}\begin{bmatrix}q_1\\q_2\\q_3\\q_4\end{bmatrix}, \tag{5}$$

where $\mu=\Omega_x$ and $\eta=\Omega_y$. (We have omitted the cell index *c* and the argument $\boldsymbol{\Omega}$.) Alternatively, equation (5) can be written in slope-and-average form as defined in Eqs. (42)–(45) of Adams [2], with the following values for the "lumping" parameters:

$$\theta_x=\theta_y=3,\quad \gamma_x=\gamma_y=1,\quad \textit{and}\quad \delta_x=\delta_y=2. \tag{6}$$

2.2 PWL Discontinuous (PWLD) FEM for Transport with Quadrilateral Cells

Here we present PWL basis functions for quadrilateral cells. We first define the within-cell point *c* as defined in equation (1). [In our numerical tests we use $\alpha_{c,j}$ = 1/4 for all *c* and *j*.] We then divide cell *c* into triangular sub-cells as shown in Figure 3. Now PWLD basis functions $b_{c,j}(x,y)$ can be constructed as a combination of four planes that are linear in each sub-cell and pass through unity at its support vertex *j*, $\alpha_{c,j}$ at within-cell point *c*, and zeros at three other vertices.

Then we can generate PWLD FEM equations for a given quadrilateral cell by inserting basis functions into equation (4) using Galerkin weighting. Galerkin weighting means that $w_{ci} = b_{ci}$ in Eq. (4). Integrals in equation (4) can be calculated analytically since the PWLD basis functions are linear in each sub-cell. The result is a matrix equation with four by four matrices.

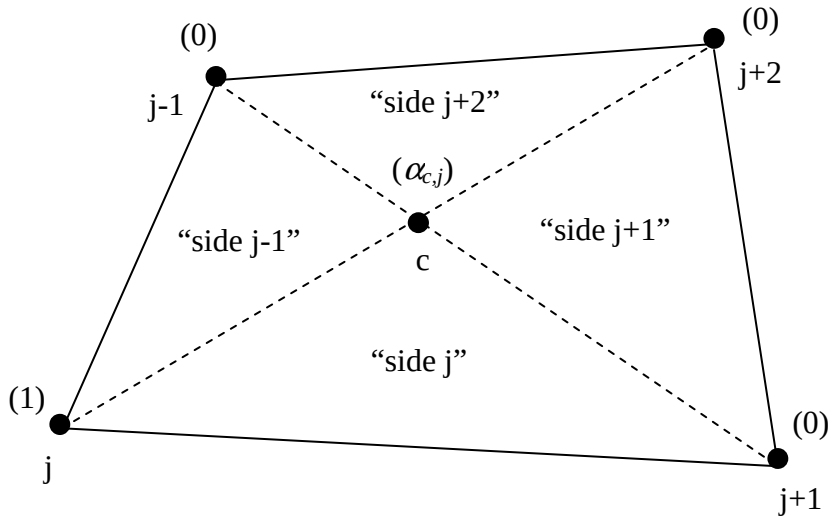

Figure 3. Illustration of a quadrilateral cell *c*. The values of the basis function $b_{c,j}(x,y)$ at vertices and the point *c* are shown in parentheses.

2.3. PWL Discontinuous (PWLD) FEM for Transport with Arbitrary Polygonal Grids

Here we present PWL basis functions on an arbitrary polygonal grid. We first define the within-cell point *c* as defined in equation (1). We then divide cell *c* into triangular sub-cells as shown in Figure 4. Now PWLD basis functions $b_{c,j}(x,y)$ can be constructed as a combination of J_c planes that are linear in each sub-cell and pass through unity at its support vertex *j*, $\alpha_{c,j}$ at within-cell point *c*, and zeros at all other vertices. Figure 4 shows the values of a basis function $b_{c,1}$(x,y) at the vertices and the within-cell point *c* in parentheses.

Equation (4) for PWLD FEM on arbitrary grids can be calculated analytically. The resulting equation can be written as a matrix equation with square matrices of order J_c.

We note here that the PWLD basis functions on any triangular cell are exactly the same as linear discontinuous basis functions. A PWL basis function is linear over entire triangular cell, not just over sub-cells, regardless of the choice of the within-cell point.

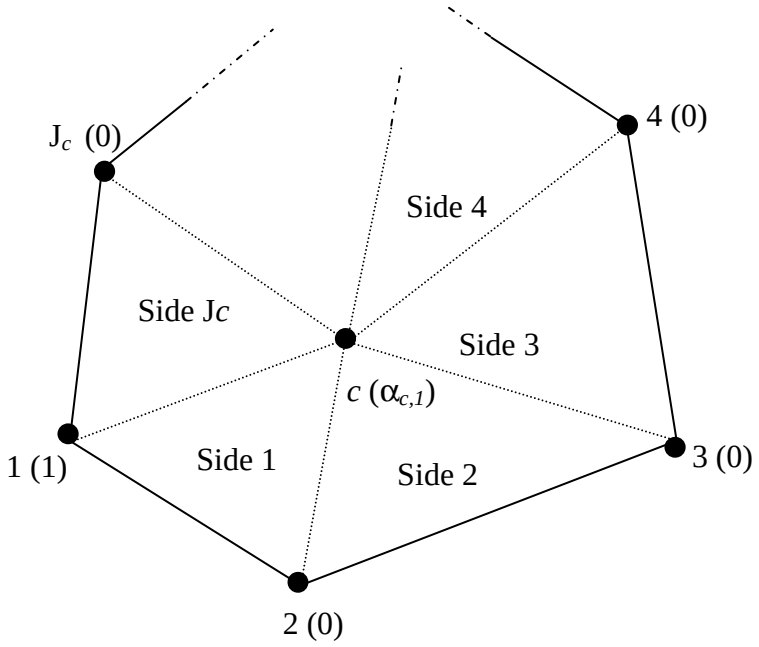

Figure 4. Illustration of an arbitrary polygonal cell *c*. The values of the basis function $b_{c,1}(x,y)$ at vertices and the point *c* are shown in parentheses.

3. BEHAVIOR IN LIMITS OF INTEREST

In this section we address the behavior of the PWLD FEM in several limits of interest. We are interested in how the solution of the PWLD FEM behaves in the fine-mesh limit, the rectangular-mesh limit, the highly distorted-mesh limit and the thick diffusive limit. We would like for the PWLD FEM solution to converge quickly to the fine-mesh solution as the grid is refined. When the grid is rectangular, we want the PWLD FEM to behave as well as well-established methods, such as the bilinear discontinuous (BLD) method. We also want the method to be as insensitive as possible to the shape of the grid cells. Finally, in the thick diffusive limit, it is desirable that the leading-order solution of the method satisfies some form of a discretized diffusion equation since the exact solution to transport problem approaches the diffusion equation in the diffusive limit.

In the rectangular-mesh limit, the PWLD method is almost identical to the standard BLD method, which is a well-known, well-studied and well-tested method. We can see this by comparing the two sets of DFEM equations; the only difference is in the *xy*-moment equation and only by a factor of 2/3 in its leakage term [2]. Our numerical test results show that this difference does not make the solution better or worse: PWLD performs just as well as BLD on rectangular grids [2].

We now address the behavior of PWLD FEM in the fine-mesh limit. If in the fine-mesh limit a grid's cells become rectangular, then PWLD becomes almost identical to rectangular-cell BLD,

which is known to be third-order accurate given smooth solutions. If the grid cells do not become rectangular in the fine-mesh limit, this relationship to BLD does not apply. However, because any linear solution can be represented by PWL basis functions on any grid, the method is exact if the angular intensity is a linear function of x and y, regardless of the cell shapes. Given a Taylor-series expansion of the angular flux, PWLD will exactly capture the constant and linear terms. This does not prove second-order truncation error, but it suggests that we might expect such truncation error. Our numerical results, presented in the section 4.1, show convergence as the grid is refined that does not depend on how distorted the grid is, even when the grid lacks smoothness. The rate of convergence is similar for three types of grids: rectangular, quadrilateral, and randomized quadrilateral. Further theoretical and numerical results are needed, but these preliminary observations suggest that PWLD behaves as well in the fine-mesh limit on unstructured grids as well-established methods do on structured grids.

We now discuss the behavior of PWLD FEM in the limit of a highly distorted mesh. We again note that no matter how distorted the grid, the method is exact if the angular intensity is a linear function of position. This gives the method a great deal of insensitivity to the grid, especially if the grid resolves solution gradients. Our Z-mesh and N-mesh test problems (Sec. 4.2) bear this out: the method is less sensitive to grid distortion than is another established method for arbitrary grids, the UCB method [4].

Finally, we address the asymptotic analysis of PWLD FEM in the "thick diffusive" limit, in which each cell becomes optically thick and dominated by scattering interactions [3]. We first note that PWLD FEM meets the sufficient conditions for a "full-resolution" method on any polygonal grid or polyhedral grid. We refer to Adams [4] for a precise definition, but in short, a "full-resolution" method means that a discontinuous FEM (DFEM) has the potential to generate reasonable solutions in thick diffusive problems. Our analysis, which follows the general analysis of Ref. [3], further shows that the leading-order PWLD solution satisfies a weighted-residual discretization of the diffusion equation written in P_1 form (i.e., written as coupled first-order differential equations). There is a weighted balance equation centered at each vertex in the problem, and weighted integrals of Fick's Law in each cell in the problem, as shown below. From the asymptotic analysis of a full-resolution DFEM in general [3], we can obtain the following equation for the leading-order solution:

$$-\int_{\mathbb{V}} d\mathbf{r}\, \boldsymbol{\nabla} v_p(\mathbf{r}) \bullet \mathbf{J}(\mathbf{r}) + \int_{\mathbb{V}} d\mathbf{r}\; v_p(\mathbf{r}) \sigma_a(\mathbf{r}) \phi(\mathbf{r}) = \int_{\mathbb{V}} d\mathbf{r}\; v_p(\mathbf{r}) q_{ext}(\mathbf{r}), \tag{7}$$

where

$$\phi(\mathbf{r}) = \sum_{j=1}^{Jc} \phi_{cj} b_{cj}(\mathbf{r}) \;,\; \mathbf{J}(\mathbf{r}) = \sum_{j=1}^{J_c} \mathbf{J}_{cj} b_{cj}(\mathbf{r}) \text{ and } v_p(\mathbf{r}) \equiv \text{ linear conbination of } \left\{ w_{ci} \right\}. \tag{8}$$

Equation (7) tells us that the leading-order solution of a full-resolution DFEM in the diffusive limit satisfies the particle balance equation in the weighted residual sense. Furthermore, if we assume continuous boundary conditions, which lead to continuous scalar intensities in the problem interior [3], we can obtain the following equation with the definitions in equation (8) for $\phi(\mathbf{r})$ and $\mathbf{J}(\mathbf{r})$:

$$\int_{\mathbb{V}} dxdy\, w_{ci}(\mathbf{r})\,\sigma(\mathbf{r})\,\mathbf{J}(\mathbf{r}) = -\frac{1}{3}\int_{\mathbb{V}} dxdy\, w_{ci}(\mathbf{r})\,\nabla\phi(\mathbf{r}) \tag{9}$$

Equation (9) tells us that the leading-order solution of a full-resolution DFEM in the diffusive limit satisfies the Fick's law in the weighted residual sense on any polygonal grid. Since the PWLD FEM is a full-resolution method, the leading-order solution of PWLD FEM satisfies equations (7) and (9).

It is interesting to note that for PWLD, Eqs. (7)-(9) do not collapse into the PWL continuous FEM discretization of the diffusion equation; there are small differences in the weightings of different flux values in the leakage term. The source of the difference, fundamentally, is that the gradient of a PWL function in a cell is not itself a combination of PWL functions. [The Wachspress rational (WR) functions do have gradients that are combinations of the rational functions in a given cell; thus the leading-order WR discontinuous solution will satisfy the continuous WR discretization of the diffusion equation under the conditions assumed here.] Different does not mean worse; in fact, given rectangular cells the leakage discretization satisfied by the leading order PWLD solution is arguably better than that of the PWL continuous discretization. Thus, we do not expect the PWLD solution to be inaccurate; it is simply slightly different from the PWLC diffusion solution. We conclude that the thick diffusive limit, the PWLD solution should behave as well on unstructured grids as the BLD solution does on grids with rectangular cells.

4. NUMERICAL RESULTS

In this section we present the results of two families of numerical tests of PWLD FEM on quadrilateral grids, comparing against well-established methods.

4.1. Mesh-Refinement Problem

Our first test problem is taken from Adams [4]. This problem tests the performance of methods as the mesh is refined. The problem is described in Figure 5. We compute the exiting flow rate from the top right quarter of the problem for various mesh refinements. This exiting flow rate is the exiting partial current density integrated over the right half of the top surface and top half of the right surface.

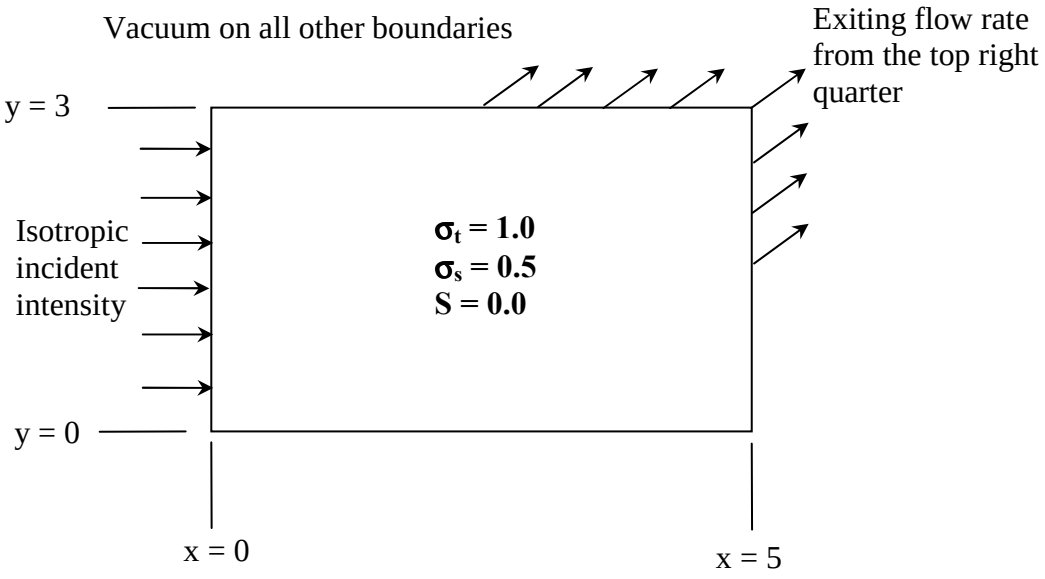

Figure 5. Description of the mesh-refinement problem.

We compare the results from the bilinear discontinuous (BLD) and PWLD FEMs on rectangular grids as well as the upstream corner balance method (UCB) [4] and PWLD FEM on smooth and randomized quadrilateral grids. Uniform cell sizes are used for test problems with rectangular grids. Examples of quadrilateral grids are shown in Figure 6. Results are presented in Table I.

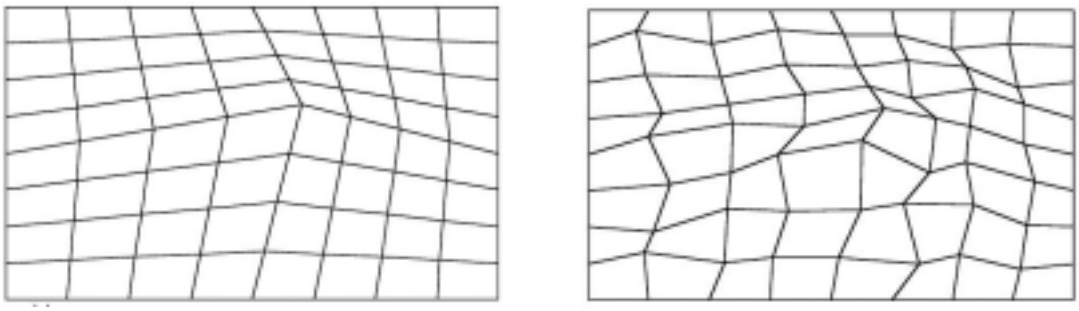

(a). Smooth quadrilateral grid (8 x 8)

(b). Randomized quadrilateral grid (8 x 8)

Figure 6. Examples of structured and smooth quadrilateral grids for mesh-refinement problem.

Table I. Exiting flow rates from the mesh-refinement problem.

Number of cells	BLD	PWLD			UCB	
	Rectangular	Rectangular	Quadrilateral	Randomized	Quadrilateral	Randomized
2 x 2	-0.011227	-0.011001	N/A	N/A	0.056656	N/A
4 x 4	0.023042	0.023015	0.021888	0.021332	0.030533	0.031036
8 x 8	0.025804	0.025800	0.025699	0.025649	0.026357	0.026336
16 x 16	0.025982	0.025982	0.025973	0.025984	0.026083	0.026157
32 x 32	0.026034	0.026034	0.026034	0.026034	0.026052	0.026082

From the results, we can see that PWLD on rectangular grids performs as well as BLD on the same grids. In fact the results are virtually identical for practical purposes. We can also say that for quadrilateral grids PWLD performs at least as well as UCB. For quadrilateral grids, while PWLD approaches the fine mesh solution from underestimated values, UCB approaches the fine mesh solution from overestimated values, with similar error magnitudes. We also see that PWLD is almost as accurate on distorted grids, even those without smooth mesh lines, as it and BLD are on grids of rectangles.

4.2. Z-mesh Problem

For our second quadrilateral grids test problem, we consider a source-free square 1 cm in width. Cross sections are chosen so that the width of the problem is approximately five diffusion lengths long with varying values for scattering ratio *c*. [The diffusion length is the inverse of the square root of $3\times\sigma_t\times\sigma_a$.] We solve this problem on a series of "Z-mesh" grids [5]. The grid description is shown in Figure 7. The distortion parameter α is defined to be the y coordinate of the lower three circled points. We vary α between 0.05 cm and 0.5 cm. The values in parentheses are number of grid divisions in the given regions. When α = 0.5 cm, the grid consists of ten by ten square cells; when it is small the grid becomes increasingly distorted. We impose reflective boundaries on the right and the left sides of the problem, with vacuum on the top boundary and an isotropic incident flux on the bottom boundary.

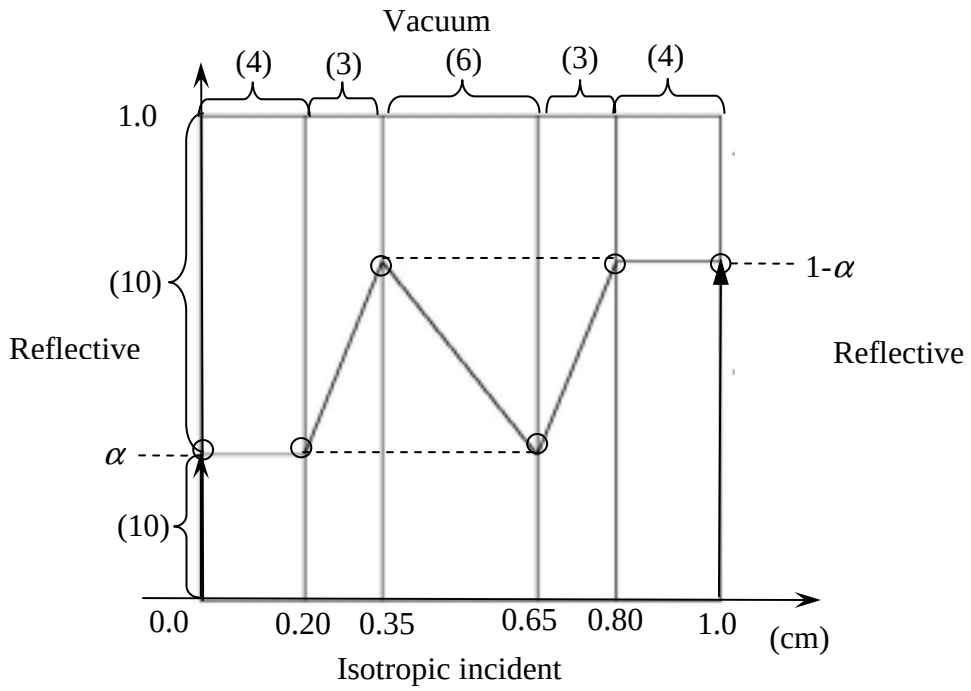

Figure 7. Description of Z-mesh test problem.

We solve this problem with PWLD and UCB, and compare their results. Since this is essentially a one-dimensional problem in the *y* variable, we would expect the solution to be independent of *x* coordinate. In fact, both PWLD and UCB produce such results when $\alpha = 0.5$ cm as shown in Figure 8. However, distortion in the grid leads to distortion of contours in the results. Figure 9 shows the test grids with $\alpha = 0.05$ cm and $\alpha = 0.3$ cm. We present contour plots of the results with $c = 0.5$ in Figure 10 and Figure 11 for PWLD and UCB, respectively.

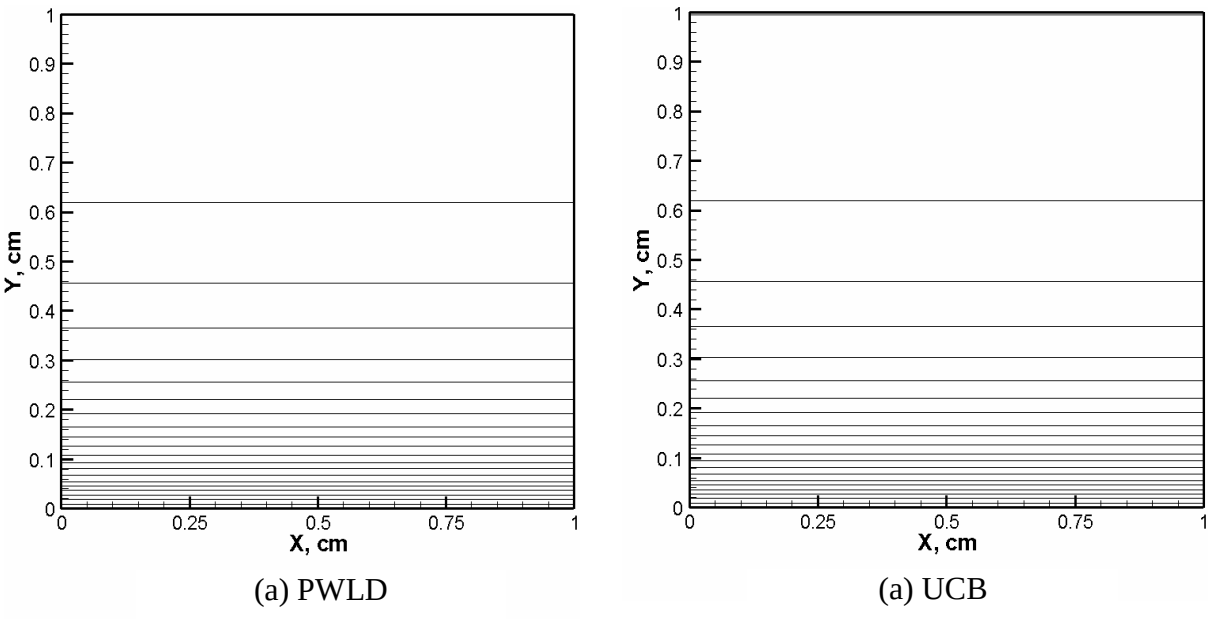

(a) PWLD (a) UCB

Figure 8. Contour plots of the results with α = 0.5 cm and c = 0.5. Contours are equally spaced on a linear scale.

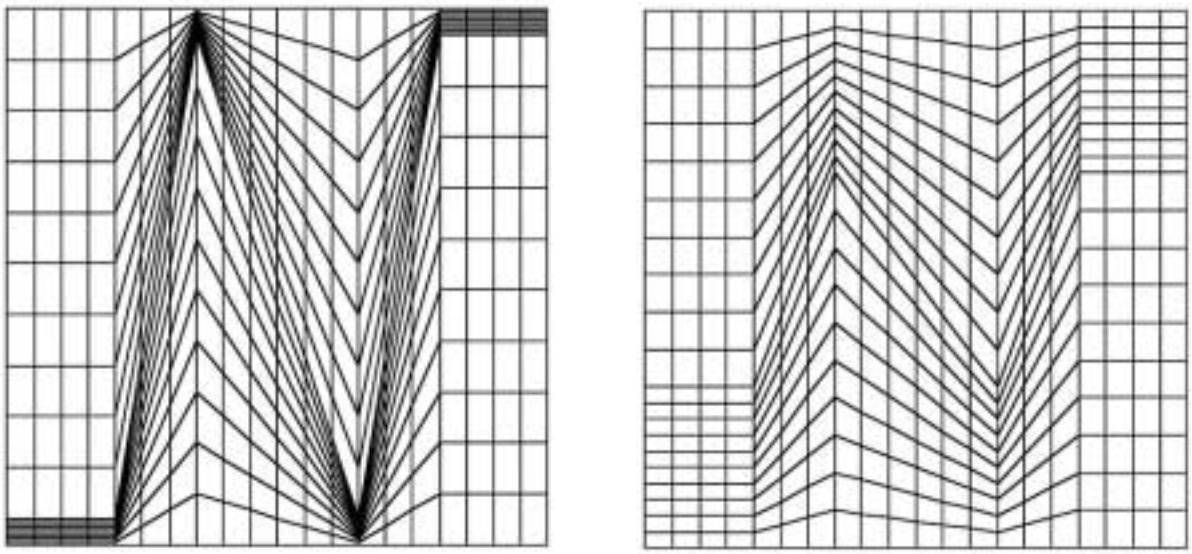

(a) α = 0.05 (b) α = 0.3

Figure 9. Spatial grids for Z mesh test problem.

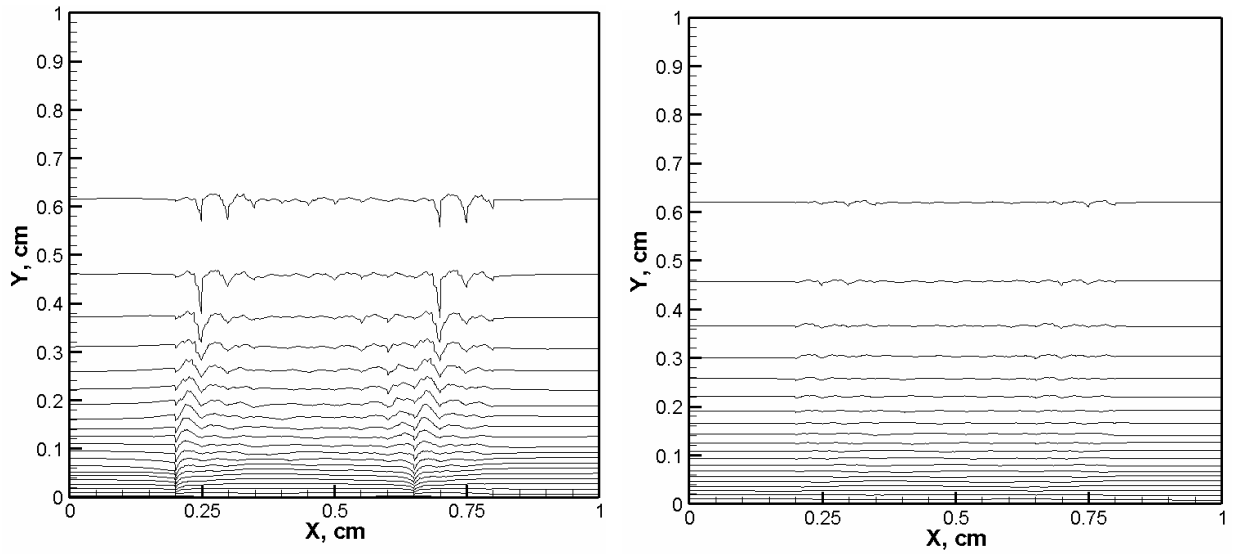

(a) $\alpha = 0.05$ (b) $\alpha = 0.3$

Figure 10. Contour plots of PWLD results for Z mesh test problem with c = 0.5.

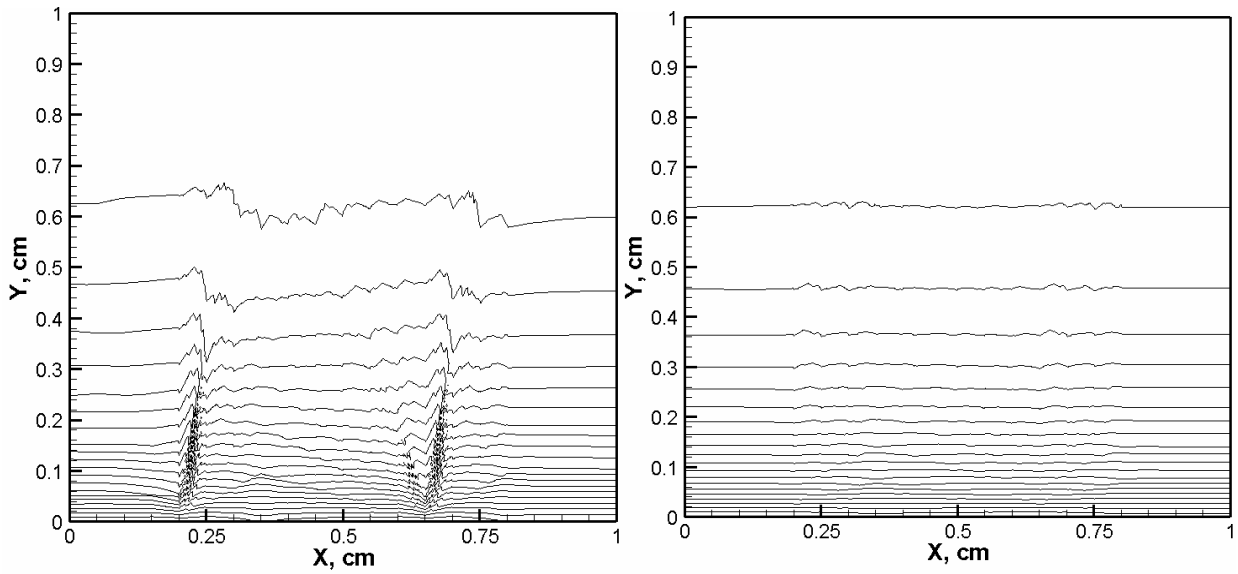

(a) $\alpha = 0.05$ (b) $\alpha = 0.3$

Figure 11. Contour plots of UCB results for Z mesh test problem with c = 0.5.

We see clearly from Figure 10 and Figure 11 that distortion in the solution contours is more severe for the smaller distortion parameter. We can also see that distortion in PWLD result is significantly less severe than distortion in UCB result, especially for $\alpha = 0.05$, which is the most

difficult problem. We observed similar results for the test problem with various values of *c*. These test results show that PWLD is less sensitive to the grid than UCB.

We also performed "N-mesh" test problem, in which the reflective boundaries are imposed on the top and bottom boundaries, vacuum on the right boundary and isotropic incident on the left boundary. For N-mesh problem, we did not observe any distortion in solution contours for various values of α and *c*. Instead, the PWLD method obtained the correct 1D solution (the solution of the 1D linear discontinuous (LD) method), just as it did on a grid of square cells. This is because on the N mesh the grid is distorted by simply sliding vertices along solution contours instead of across them. This means that the PWLD solution values at a given vertex have no reason to change from their square-cell or 1D values.

5. SUMMARY AND CONCLUSIONS

We have developed a piecewise linear (PWL) finite element basis function that can be applied to the arbitrary polygonal or polyhedral grids. We have used the PWL discontinuous (PWLD) basis functions in the discontinuous finite element method (DFEM) transport equation. We have analyzed the resulting method for polygonal cells and implemented it on rectangular and quadrilateral grids in 2D problems with Cartesian coordinate systems. On rectangular grids, we have compared the PWLD FEM analytically and numerically against the bilinear discontinuous (BLD) FEM. On quadrilateral grids, we have compared the method against the upstream corner balance (UCB) method.

Our analyses and numerical tests have shown that the PWLD solution converges to the fine-mesh solution as the grid is refined, even for distorted grids that lack smooth mesh lines. PWLD FEM performs as well as BLD on rectangular grids, and at least as well as UCB on quadrilateral grids. PWLD FEM has greater insensitivity to distortions in the grid than UCB does.

We conclude that PWLD is a promising method for transport calculations on unstructured spatial grids. In the future we expect to implement and test PWLD for arbitrary polygonal cells in 2D and for polyhedral cells in 3D. We also plan to implement a robust, rapidly convergent iterative method that will allow us to test problems with optically thick, highly scattering regions.

REFERENCES

1. E. L. Wachspress, *A Rational Finite Element Basis*, Academic Press, New York (1975).
2. H. G. Stone and M. L. Adams, "A Piecewise Linear Finite Element Basis with Application to Particle Transport," *Transactions of American Nuclear Society Winter Meeting*, Washington, D.C., November 17-21, 2002, Vol. 87, pp. 130-133 (2002).
3. M. L. Adams, "Discontinuous Finite Element Transport Solutions in Thick Diffusive Problems," *Nuclear Science and Engineering*, **137**, pp.298-333 (2001).
4. M. L. Adams, "Subcell Balance Methods for Radiative Transfer on Arbitrary Grids," *Transport Theory and Statistical Physics*, **26(4&5)**, pp.385-431 (1997).
5. T. S. Palmer, *Curvilinear Geometry Transport Discretizations in Thick Diffusive Regions*, University of California Lawrence Livermore National Laboratory, Livermore, CA (1993).